



Target of rapamycin signaling couples energy to oxygen sensing to modulate hypoxic gene expression in *Arabidopsis*

Alicja B. Kunkowska^a, Fabrizia Fontana^a, Federico Betti^a, Raphael Soeur^b, Gerold J. M. Beckers^b, Christian Meyer^c, Geert De Jaeger^{d,e}, Daan A. Weits^{a,f,g}, Elena Loreti^{h,1}, and Pierdomenico Perata^{a,1}

Edited by Julia Bailey-Serres, University of California, Riverside, CA; received July 27, 2022; accepted December 6, 2022

Plants respond to oxygen deprivation by activating the expression of a set of hypoxia-responsive genes (HRGs). The master regulator of this process is a small group of transcription factors belonging to group VII of the ethylene response factors (ERF-VIIs). ERF-VIIs are highly unstable under aerobic conditions due to the continuous oxidation of their characteristic Cys residue at the N terminus by plant cysteine oxidases (PCOs). Under hypoxia, PCOs are inactive and the ERF-VIIs activate transcription of the HRGs required for surviving hypoxia. However, if the plant exposed to hypoxia has limited sugar reserves, the activity of ERF-VIIs is severely dampened. This suggests that oxygen sensing by PCO/ERF-VII is fine-tuned by another sensing pathway, related to sugar or energy availability. Here, we show that oxygen sensing by PCO/ERF-VII is controlled by the energy sensor target of rapamycin (TOR). Inhibition of TOR by genetic or pharmacological approaches leads to a much lower induction of HRGs. We show that two serine residues at the C terminus of RAP2.12, a major ERF-VII, are phosphorylated by TOR and are needed for TOR-dependent activation of transcriptional activity of RAP2.12. Our results demonstrate that oxygen and energy sensing converge in plants to ensure an appropriate transcription of genes, which is essential for surviving hypoxia. When carbohydrate metabolism is inefficient in producing ATP because of hypoxia, the lower ATP content reduces TOR activity, thus attenuating the efficiency of induction of HRGs by the ERF-VIIs. This homeostatic control of the hypoxia-response is required for the plant to survive submergence.

hypoxia | *Arabidopsis* | TOR

Plants exposed to low oxygen availability rapidly face an energy crisis (1–5). When the oxygen level falls below that required for oxidative phosphorylation in the mitochondrion, energy production is reduced from the 36 moles of adenosine triphosphate (ATP) per mole of glucose to only two, assuming that glycolysis occurs coupled with ethanol fermentation to recycle the nicotinamide adenine dinucleotide required for continued glucose oxidation under hypoxia (5). ATP production via the fermentative metabolism is crucial for survival, and mutants for both pyruvate decarboxylase (PDC) and alcohol dehydrogenase (ADH1) are hypoxia intolerant (6–8). Starch is also important for survival, given that it provides long-term sugar availability to fuel glycolysis coupled with fermentation (9).

The shift from aerobic mitochondrial respiration to anaerobic metabolism requires the induction of several glycolytic and fermentative enzymes (5), which are produced after sensing an oxygen-poor environment (10). Oxygen sensing occurs via the stabilization of oxygen-labile transcription factors belonging to the group VII ethylene response factors (ERF-VII) in a mechanism that also involves nitric oxide and ethylene (11–14). ERF-VIIs possess a Cys residue at the N terminus, which under aerobic conditions is oxidized enzymatically by the action of plant cysteine oxidases (PCOs) (15). Under hypoxia, ERF-VIIs transcriptionally activate several genes, including those involved in carbohydrate metabolism, glycolysis, and fermentation.

Interestingly, the initial drop in ATP content experienced in the hypoxic cell promotes the activity of ERF-VII. This occurs by reducing long-chain acyl-CoA synthetase activity, which results in a change in the composition of the acyl-CoA pool, leading to the release of the ERF-VII transcription factor RAP2.12 from its interaction partner acyl-CoA-binding protein at the plasma membrane (16). Subsequently, oxygen concentration-dependent stabilization of ERF-VIIs determines the level of hypoxia-specific gene expression.

The induction of hypoxia-responsive genes (HRGs) can take place even within 30 min of the onset of hypoxia, and typically peaks after 4 to 5 h (17–20). Subsequently, the expression of HRGs is dampened, presumably to ensure a homeostatic control of the rate of carbohydrate consumption thereby securing long-lasting energy production in the plants suffering from submergence-induced hypoxia (9). Residual carbohydrate availability is essential to ensure post-submergence recovery when the water recedes, both in rice and *Arabidopsis* (9, 21).

Significance

Plants need oxygen for their energy metabolism. Flooding events limiting oxygen availability are more frequent due to climate change and impact negatively on plant growth and productivity. Under hypoxia, a small group of transcription factors, named ERF-VIIs, are stabilized and activate hypoxia-responsive genes (HRGs) which helps the plant adapt to hypoxia. However, sugar and energy starvation considerably inhibit the induction of HRGs. How energy availability influences the transcriptional consequences of oxygen sensing is unknown. Here, we demonstrate that oxygen sensing by ERF-VIIs is fine-tuned by target of rapamycin (TOR) kinase, a master energy sensor widely conserved in all eukaryotes. Our study revealed that only under optimal energy availability does TOR activate ERF-VIIs, demonstrating a cross-talk between oxygen and energy sensing.

Author contributions: A.B.K., F.F., E.L., and P.P. designed research; A.B.K., F.F., F.B., R.S., G.J.M.B., and D.A.W. performed research; C.M. and G.D.J. contributed new reagents/analytic tools; A.B.K., F.F., G.J.M.B., D.A.W., E.L., and P.P. analyzed data; and A.B.K., E.L. and P.P. wrote the paper.

The authors declare no competing interest.

This article is a PNAS Direct Submission.

Copyright © 2023 the Author(s). Published by PNAS. This open access article is distributed under [Creative Commons Attribution-NonCommercial-NoDerivatives License 4.0 \(CC BY-NC-ND\)](https://creativecommons.org/licenses/by-nc-nd/4.0/).

¹To whom correspondence may be addressed. Email: loreti@ibba.cnr.it or p.perata@santannapisa.it.

This article contains supporting information online at <https://www.pnas.org/lookup/suppl/doi:10.1073/pnas.2212474120/-DCSupplemental>.

Published January 10, 2023.

A mechanism reducing the action of ERF-VII has been discovered, which is based on the action of a trihelix protein, named the hypoxia-response attenuator (HRA1) (22). HRA1 binds to RAP2.12 and reduces its activity. HRA1 is itself a product of ERF-VII transcriptional activation and acts as a feedback control for the hypoxic response (11). However, a plant may experience hypoxia with low carbohydrate reserves, such as when submergence occurs after prolonged exposure to darkness or in starch-defective mutants. In such cases, early on the induction of HRGs is severely reduced in an HRA1-independent manner (9).

The lower production of enzymes needed for glycolysis and fermentation when sugars in the plant are unavailable is a conservative response that reduces ATP consumption to produce enzymes that would not otherwise have enough substrates to offset the cost of their own synthesis (23). Neither HRA1 nor SNF1-related protein kinase (SnRK1), a regulator of carbohydrate metabolism and energy balance, is involved in the carbon-starvation-dependent dampening of the hypoxic response (9). It is thus currently unknown how, when hypoxia is detected, plants monitor sugar availability to ensure an advantageous metabolic result after vigorous transcription of glycolytic and fermentative enzymes.

Perceiving nutrient and energy levels inside and outside the cell is crucial to adjust growth and metabolism to available resources (24). Signaling pathways based on the conserved target of rapamycin (TOR) and SnRK1/Snf1/AMPK kinases play an essential role for energy sensing in the cell and in translating this information into metabolic and developmental adaptations (24). In Arabidopsis, just one *TOR* gene is present. Components of TOR complex 1 (TORC1) partners have been identified, including the lethal with sec thirteen 8 (LST8) and regulatory-associated protein of TOR (RAPTOR) proteins (25).

Here, we show that plants exploit the TOR pathway to ensure that the hypoxic response induced by ERF-VII matches the current energy status of the cell. If the energy status of a cell exposed to hypoxia is low, TOR is inactive, and this leads to the reduced activity of ERF-VIIs. Both TOR and RAP2.12 are thus necessary to ensure a good coordination between the plant's energy status and the activity of the oxygen-sensing machinery.

Results

Reduced Photosynthetic or Mitochondrial Activity Prevents a Full Hypoxic Response. An extended night treatment induces carbon starvation, as indicated by the strong expression of *dark inducible 6* (*DIN6*), a sugar starvation-responsive gene (Fig. 1*A*). It also severely dampens the expression of *ADH1* and *PCO1* in adult Arabidopsis plants under submergence (Fig. 1*A*), which both usually respond vigorously to hypoxia. The same expression pattern was observed for two other HRGs, namely *HRA1* and *PGB1* (*SI Appendix, Fig. S1*). Plants that underwent submergence treatment (72 h), after 6 h of light recovered from the treatment and developed into normal, healthy plants, while plants that underwent submergence after a 6 h long extended night treatment were unable to recover and died (Fig. 1*B*). This was confirmed in an independent experiment (*SI Appendix, Fig. S2*). To decouple darkness from sugar starvation in regulating the induction of *ADH1*, we treated adult plants kept in the light with the photosynthesis inhibitor DCMU (Fig. 1*C*). Treating plants with DCMU resulted in a strong reduction in the production of starch, which impacted on the light-dependent availability of glucose under hypoxia (*SI Appendix, Fig. S3A*). The induction of *ADH1* by hypoxia was very strong in plants that were light-treated, whereas it was almost totally repressed in plants that underwent extended night treatment (Fig. 1*D*) (9). The negative impact of darkness was

also observed on a set of additional hypoxia-regulated genes, which includes *PCO1*, *PGB1*, and *HRA1*, all three encoding hypoxic proteins with a regulatory role (*SI Appendix, Fig. S4*).

Interestingly, DCMU treatment on light-treated plants repressed the hypoxic induction of *ADH1* and of the other HRGs tested at the same level as dark-treated plants (Fig. 1*D* and *SI Appendix, Fig. S4*). Repression of *ADH1* in extended night-treated plants is thus not darkness driven but induced by reduced sugar production by photosynthesis. In fact, expression of *DIN6*, a carbon starvation marker, was strongly induced by DCMU, irrespectively of light. This confirms the induction of carbon starvation by the photosynthesis inhibitor (Fig. 1*D*).

Given that treatment in the dark leads to a fall in ATP content under both air and hypoxia (Fig. 1*E*), we investigated whether the reduced induction of HRGs in dark-pretreated plants could be related to a low ATP level. When plants were treated with DCMU, we observed a drop in ATP content under hypoxia (Fig. 1*E*). We therefore treated adult plants with oligomycin, an inhibitor of ATP synthase, to reduce the ATP content in plants (Fig. 1*F*). When plants grown in the light were treated with oligomycin, the hypoxia induction of *ADH1* was then completely blocked (Fig. 1*G*). The hypoxic induction of *PCO1*, *HRA1*, and *PGB1* was repressed by oligomycin at the same level as that of dark-treated plants (*SI Appendix, Fig. S5*). The results also showed that oligomycin decreased ATP content even in light-grown hypoxic plants (Fig. 1*H*). Oligomycin did not impact on the ability of the plant to produce starch, and exerted a minor effect on the level of sugars, both under hypoxia in the plants from light and dark (*SI Appendix, Fig. S3B*). Taken together, these results indicated that the darkness-induced dampening of the hypoxic response is due to sugar starvation leading to a reduction in ATP content (Fig. 1 *E–H*).

TOR Is Required for a Complete Transcriptional Response to Hypoxia. The conserved TOR and SnRK1 protein kinases are central hubs that coordinate cellular adaptations to changes in nutrient and energy status (24, 26). We previously demonstrated that sugar starvation dampens the hypoxic response independently of HRA1, the SnRK1 protein KIN10, and bZIP63 (9). We therefore focused on TOR. We tested if a prolonged night treatment prior to 4-h dark-submergence results in TOR being less able to phosphorylate ribosomal protein S6 (RPS6), a well-known TOR substrate (27). This was demonstrated by western blotting using two different antibodies against RPS6, either against phosphorylated protein (α -P-RPS6; showing reduction of TOR activity of RPS6 as a substrate) or total protein (α -RPS6), the latter was utilized as a loading control.

The results demonstrated that TOR activity is severely dampened by an extended night treatment, as indicated by the greatly reduced phosphorylation of RPS6 (α -P-RPS6) (Fig. 2*A*). We performed a time-course of TOR activity during a 10-h submergence treatment in the dark, using plants that were light-pretreated, to understand if the decline in HRGs expression occurring after 4 h of submergence (Fig. 1*A*) could be related to the activity of TOR. TOR activity indeed showed a rapid, but gradual, decline of activity during submergence (Fig. 2*B*). The quantitative analysis of replicated, independent western blots (WBs) (Fig. 2*B*) indicated that TOR activity is significantly repressed after 2 h of submergence, as shown by the decreased level of phosphorylated RPS6 protein (Fig. 2*B*). The total amount of RPS6 protein did not change during the experiment (Fig. 2*C*). The expression of HRGs peaks 4 h into the submergence treatment, but decreases thereafter (Fig. 1*A*). Interestingly, while soluble sugars did not decrease earlier than after 6 h of submergence (Fig. 2*D* and *SI Appendix, Fig. S6*), the ATP content was lower

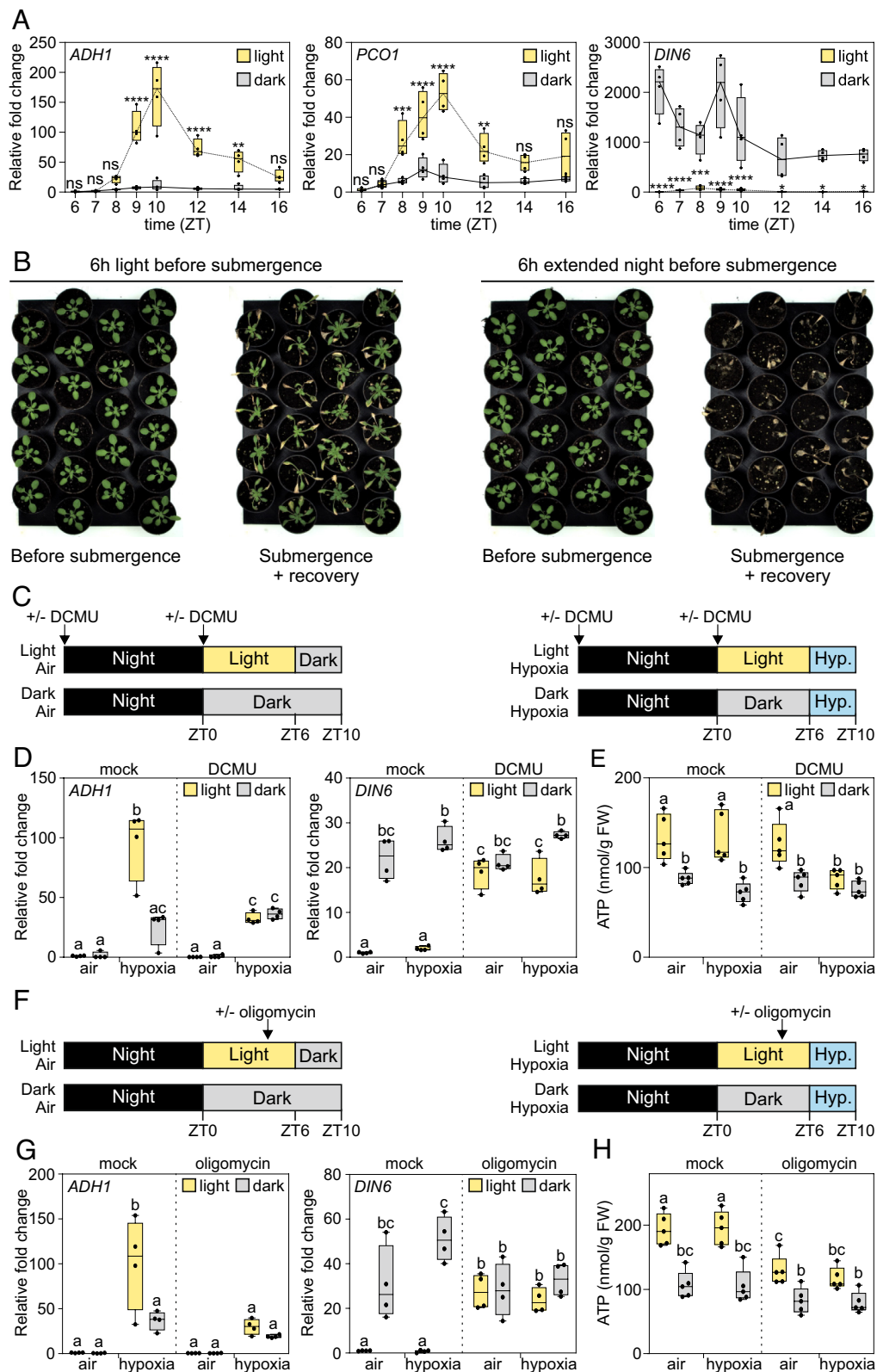


Fig. 1. Reduced ATP content dampens hypoxic responses in *Arabidopsis thaliana*. (A) Relative fold change of *ADH1*, *PCO1*, and *DIN6* expression in WT plants after a 6-h pretreatment in either light or dark. Data were collected in air (ZT6) and after 1 to 10 h of submergence in the dark. (B) Phenotypes of WT plants which underwent a 6-h pretreatment in either light or dark (extended night), before 3 d of submergence. Photographs were taken 1 d before the pretreatment and after 10 d of recovery. *SI Appendix, Fig. S2* contains a graph showing survival percentage assessed after 10 d of recovery. (C) The experimental set-up used in D and E. (D) Relative fold change of *ADH1* and *DIN6* expression in WT plants after a 6-h pretreatment in either light or dark, followed by 4 h of hypoxia or air, coupled with DCMU treatment, following the experimental set-up from C. (E) ATP levels in Col-0 plants after a 6-h pretreatment in either light or dark, followed by 4 h of hypoxia or air, coupled with DCMU treatment, following the experimental set-up from C. (F) The experimental setup used in G and H. (G) The same as in D, but with oligomycin treatment, following the experimental setup from F. (H) The same as in E, but with oligomycin treatment, following the experimental set-up from F. All data are expressed as relative to the expression levels detected under air/light conditions. A, D, and G, $n = 4$ biological replicates; E and H, $n = 5$ biological replicates. In the boxplots, dots represent single data points, whiskers denote the minimum/maximum values, the box defines the interquartile range, the center represents the median, and box borders represent the lower and upper quartiles. Asterisks indicate statistically significant differences as assessed by ANOVA tests (Sidak's post hoc test, $P < 0.05$). Different letters (a, b, c, ac, bc) indicate differences in ANOVA tests (Tukey's post hoc test, $P < 0.05$).

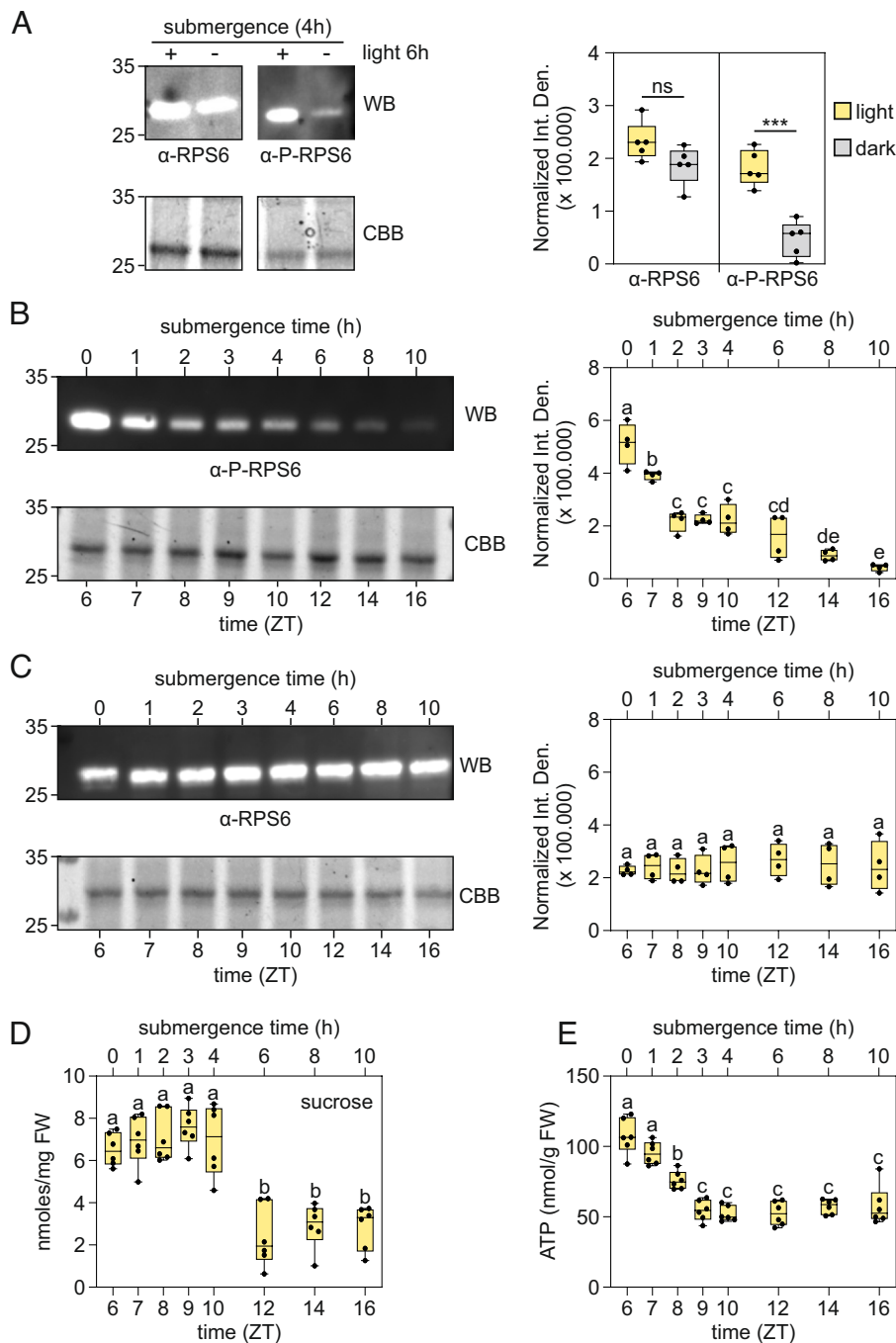


Fig. 2. TOR activity gradually decreases throughout submergence. (A) Representative WBs probed with a phospho-specific antibody recognizing phosphorylated RPS6 (α -P-RPS6), or an antibody against total RPS6 (α -RPS6). Total protein extracts were obtained from 4-wk-old WT plants after a 6-h pretreatment in either light or dark, followed by 4 h of submergence. Coomassie brilliant blue (CBB) staining was used to test for equal loading. The graph shows the quantification of normalized integrated density of WB bands from five independent experiments. ImageJ software was used to quantify the band intensities. All the original WB used for integrated density quantification are provided in *SI Appendix, Fig. S20A*. (B) Representative WB with an α -P-RPS6 antibody. Total protein extracts were obtained from 4-wk-old Col-0 plants after a submergence treatment for 0 h, 1 h, 2 h, 3 h, 4 h, 6 h, 8 h, or 10 h. Prior to stress, plants were kept under normal light conditions for 6 h. CBB was used to test for equal loading. The graph shows the quantification of normalized integrated density of WB bands, performed in ImageJ software. All original WB used for integrated density quantification are provided in *SI Appendix, Fig. S20B*. (C) The same as in A, but WB was performed with an α -RPS6 antibody. (D) Sucrose content in 4-wk-old WT plants after a submergence treatment as described in B. Prior to stress, plants were kept under the normal light conditions for 6 h. (E) The same as in D but the ATP levels were measured. A, $n = 5$ biological replicates; B and C, $n = 4$ biological replicates; D and E, $n = 6$ biological replicates. In the boxplots, dots represent single data points, whiskers denote the minimum/maximum values, the box defines the interquartile range, the center represents the median, and box borders represent the lower and upper quartiles. Asterisks indicate statistically significant differences as assessed by Student's t test ($P < 0.05$). Different letters (a, b, c, e, ac, cd, de) indicate differences in ANOVA tests B, C, E (Tukey's post hoc test, $P < 0.05$) D (Sidak's post hoc test, $P < 0.05$).

under submergence as early as after 2 h of submergence (Fig. 2E), with a gradual decline in the amount of ATP between 0 and 4 h of submergence, which correlates well with TOR activity under submergence (Fig. 2B). On the contrary, the amount of soluble sugars

was quite stable between 0 and 4 h of submergence, and dropped sharply only at 6 h of submergence (Fig. 2D and *SI Appendix, Fig. S6*). Although merely correlative, these results suggest that it is the ATP content that modulates TOR activity rather than sugars.

We also tested whether DCMU and oligomycin exerted a negative effect on TOR activity. This was confirmed by the results, showing that both treatments lead to a marked reduction in TOR activity (*SI Appendix, Fig. S7*).

We used an Arabidopsis line in which TOR is silenced by an estradiol-inducible amiRNA (*tor-es2*). The repression of *ADH1* induction by hypoxia (vs. air) in dark-pretreated plants was evident when compared with its strong expression in light-pretreated hypoxic plants (Fig. 3A). Estradiol treatment of *tor-es2* plants resulted in the dampening of *ADH1* induction, similarly to the effect of darkness (Fig. 1A). Additionally, other HRGs were repressed when TOR was inhibited by the estradiol treatment (*SI Appendix, Fig. S8A*). The efficacy of estradiol in strongly reducing the activity of TOR was demonstrated by a WB test (*SI Appendix, Fig. S9A*). Plants underwent hypoxia, rather than submergence, to prevent estradiol washing-out from the leaves, so that its effect was prolonged for the hypoxia treatment. We confirmed that functional TOR is required during submergence using a different RNAi-inducible line (RNA interference), namely *TOR RNAi line 6-3*, in which the TOR can be silenced by treating plants with ethanol vapors. To test whether ethanol induction of TOR silencing was effective, we measured the capacity of TOR to phosphorylate RPS6 (*SI Appendix, Fig. S9B*). In this case, the ethanol vapors were already exerting their effects on the expression of TOR and plants could be fully submerged. In fact, the *TOR RNAi line 6-3* also lost the ability to respond to light as a booster of the hypoxic induction of *ADH1* (Fig. 3B and *SI Appendix, Fig. S8B*).

When light-grown adult plants were treated with AZD8055, which is a potent selective ATP-competitive TOR inhibitor (28), hypoxic induction of *ADH1* under the permissive light was severely dampened (Fig. 3C), as well as that of other HRGs (*SI Appendix, Fig. S10*). AZD8055 did not perturb *DIN6* expression under light, indicating that this inhibitor does not interfere with the sugar status of the plant (Fig. 3C).

To ensure that the observed responses were associated with carbon availability, we performed experiments using protoplasts that were air/hypoxia treated in the presence or absence of exogenous sucrose. The activity of TOR was enhanced in protoplasts treated with sucrose (*SI Appendix, Fig. S11A*). The *PCO1* promoter is strongly activated by hypoxic conditions, and *PCO1* belongs to the 49 core HRGs (18). We used a *pPCO1:FLuc* construct to examine the effects of carbon availability on the hypoxic response in protoplasts. The *PCO1* promoter was expressed at low levels in the absence of sucrose, as well as when sucrose was present at concentrations lower than 60 mM (*SI Appendix, Fig. S11B*).

A clear increase in the *PCO1* promoter activity was observed at 60 and 90 mM sucrose (*SI Appendix, Fig. S11B*). Sucrose concentrations above 90 mM inhibited *pPCO1* promoter activity (*SI Appendix, Fig. S11B*), possibly due to osmotic stress negatively impacting on TOR activity (29, 30). Both sucrose and glucose activate the expression of the *pPCO1* promoter, while mannitol is ineffective (*SI Appendix, Fig. S11C*). As expected, in an aerobic environment, no *pPCO1* activity with or without sugar was observed (Fig. 3D). Under hypoxia, the sucrose-enhanced *pPCO1:FLuc* activity was severely dampened by AZD8055 (Fig. 3D). We tested the effects of torin2, another potent TOR inhibitor (31), confirming the repression of the sucrose-dependent enhancement of *pPCO1* activity (Fig. 3E). All these results indicate that active TOR is needed to ensure the activation of the hypoxic response in Arabidopsis.

We tested whether inhibiting TOR activity increased the level of RAP2.12 as previously observed in plants exposed to prolonged darkness (9, 32). We confirmed the effect of darkness by observing increased nuclear localization of stable *35S:Δ13RAP2.12-GFP*

(Green Fluorescence Protein; *SI Appendix, Fig. S12A*). This line expresses a RAP2.12 version that lacks amino acids 1 to 13 and which is driven by the *35S* promoter (*35S:Δ13RAP2.12-GFP*).

The role of TOR is therefore independent of the N-degron pathway, as previously described for the darkness-induced effects (9). Interestingly, treatment with DCMU elicited a very similar increase in the *35S:Δ13RAP2.12-GFP* signal in the nucleus, which was reversed by adding exogenous sucrose (*SI Appendix, Fig. S12B*). Most importantly, AZD8055 also increases the nuclear localization of *35S:Δ13RAP2.12-GFP* (*SI Appendix, Fig. S12C*), thus indicating that TOR affects the nuclear localization of RAP2.12. The level of RAP2.12 in the nucleus is thus inversely correlated with its transcriptional activity as observed in darkness, DCMU, and AZD8055 experiments (Figs. 1 and 3C). A mechanism that ensures that the amount of RAP2.12 in the nucleus is related to its activation status—and not only to the stabilization of the protein under hypoxia—could provide a better homeostatic control of the hypoxic response.

In plants, TOR functions as a complex (TORC1) with the core components, RAPTOR and LST8 (33). We tested hypoxic responses in a mutant in all five ERF-VII proteins (*erfVII*), as well as in RAPTOR (*raptor 7-8*) and LST8 mutants (*lst8-1-1*). We transformed protoplasts from all three mutants with the *pPCO1:FLuc* construct and kept them hypoxic in order to measure induction of the *pPCO1* promoter. In wild-type (WT) protoplasts, sucrose enhanced the expression of the *pPCO1:FLuc* construct (Col-0; Fig. 4A and B). Protoplasts responded to exogenous sugars by activating TOR, with RPS6 phosphorylation as an output (*SI Appendix, Fig. S11A*). As expected, functional ERF-VII proteins are needed to induce the *pPCO1* promoter (*erfVII*; Fig. 4A and B). Remarkably, the *pPCO1* promoter was insensitive to sucrose when either *raptor 7-8* or *lst8-1-1* protoplasts were used, indicating that all components of the TOR complex are required to enable sucrose to respond to hypoxia (Fig. 4A and B). A time-course experiment using light pretreated adult Arabidopsis plants under submergence showed that *PCO1* (Fig. 4C and D) as well as several other HRGs (*SI Appendix, Fig. S13*) are less induced in *raptor 7-8* and *lst8-1-1* mutant plants than in Col-0 plants, thus indicating that the TOR complex is required for a full hypoxic response.

To verify the contribution of RAPTOR and LST8 to submergence survival, we performed a submergence tolerance experiment using mutant lines for these two components of the TOR complex. The results showed that *raptor7-8* and *lst8-1-1* plants were more sensitive to submergence than WT plants (Fig. 4E and F and *SI Appendix, Fig. S14*), confirming that the TOR complex is required for submergence tolerance.

The C Terminus of RAP2.12 Is Required for Sucrose Responsiveness and TOR-Dependent Regulation. TOR is a highly-conserved serine/threonine protein kinase (33). We mapped all the threonine and serine residues on RAP2.12 and found that two of them are located in the C-terminal activation domain of the transcription factor (Fig. 5A). We investigated the role of the two serine residues at the C terminus of RAP2.12 in the regulation by sugars. Protoplasts obtained from the leaves of the *erfVII* mutant were transformed with a full-length version of *RAP2.12* and with a truncated version of *RAP2.12* comprising the last 18 amino acids of the C terminus, fused to the GAL4 DNA-binding domain: *GAL4-DBD* (CMVII-5, Fig. 5B). The fragment 341 to 358, comprising CMVII-5, was previously shown to harbor the activity domain of RAP2.12 (34). We confirmed that activation of the *pUAS:FLuc* construct requires the full *GAL4-DBD:RAP2.12*, but also that the *GAL4-DBD:CMVII-5* construct behaves very

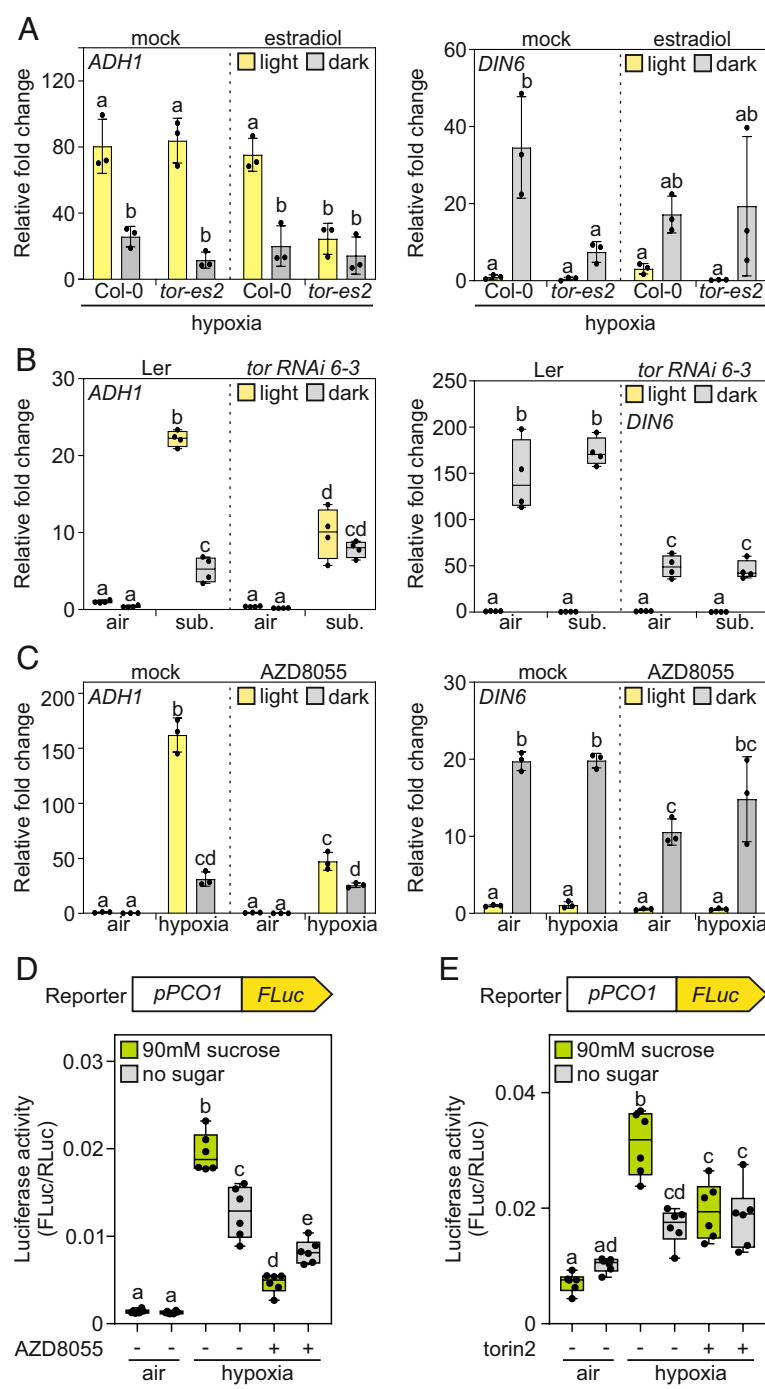


Fig. 3. Functional TOR is required for sufficient hypoxic responses. (A) Relative fold change of *ADH1* and *DIN6* expression in WT plants and *tor* estradiol-inducible mutant (*tor-es2*) after a 6-h pretreatment in either light or dark, followed by 4 h of hypoxia, coupled with estradiol treatment. Fold induction by hypoxia was calculated vs. the aerobic sample. The effectiveness of estradiol treatment on TOR activity was assessed by WB using antibodies against TOR substrate (SI Appendix, Fig. S9A). (B) Relative fold change of *ADH1* and *DIN6* expression in WT plants (Ler) and *tor* ethanol-inducible mutant (*tor RNAi 6-3*) after a 6-h pretreatment in either light or dark, followed by 4 h of submergence or air. Plants were incubated with ethanol vapors for 24 h before submergence. The effectiveness of ethanol incubation was assessed by WB using antibodies against TOR substrate (SI Appendix, Fig. S9B). (C) Relative fold change of *ADH1* and *DIN6* expression in WT plants after a 6-h pretreatment in either light or dark, followed by 4 h of hypoxia or air. AZD8055 was applied 2 h before hypoxia treatment. (D) Effect of 1 μ M AZD8055 inhibitor on wild-type protoplasts after 4-h hypoxia treatment. Half of the samples were supplied with 90 mM sucrose. (E) Same as D but with 5 μ M torin2 inhibitor. Data in A–C are expressed as relative to the expression levels detected under air/light conditions. A and C, $n = 3$ biological replicates; B, $n = 4$ biological replicates; D and E, $n = 6$ biological replicates. In the boxplots, dots represent single data points, whiskers denote the minimum/maximum values, the box defines the interquartile range, the center represents the median, and box borders represent the lower and upper quartiles. In A and C, data represent mean \pm SD, dots represent single data points. Different letters (a, b, c, d, e, ab, ad, bc, cd) indicate differences in ANOVA tests (Tukey's post hoc test, $P < 0.05$).

similarly, with a clear effect of sucrose. Remarkably, RAP2.12 lost its ability to activate *pUAS:FLuc* if the CMVII-5 domain was deleted (*RAP2.12 Δ CMVII-5*) (SI Appendix, Fig. S15). The results showed that there is no background activation of *pUAS* promoter when GAL4-DBD-GUS was used, but it was

restored in both GAL4-DBD-RAP2.12 and GAL4-DBD-CMVII-5 transformed protoplasts (Fig. 5B). Notably, the 18 amino acids at the RAP2.12 C terminus were sufficient to convey sucrose-responsiveness of the native transcription factor. The sugar effect was abolished in GAL4-DBD-CMVII-5 when AZD8055

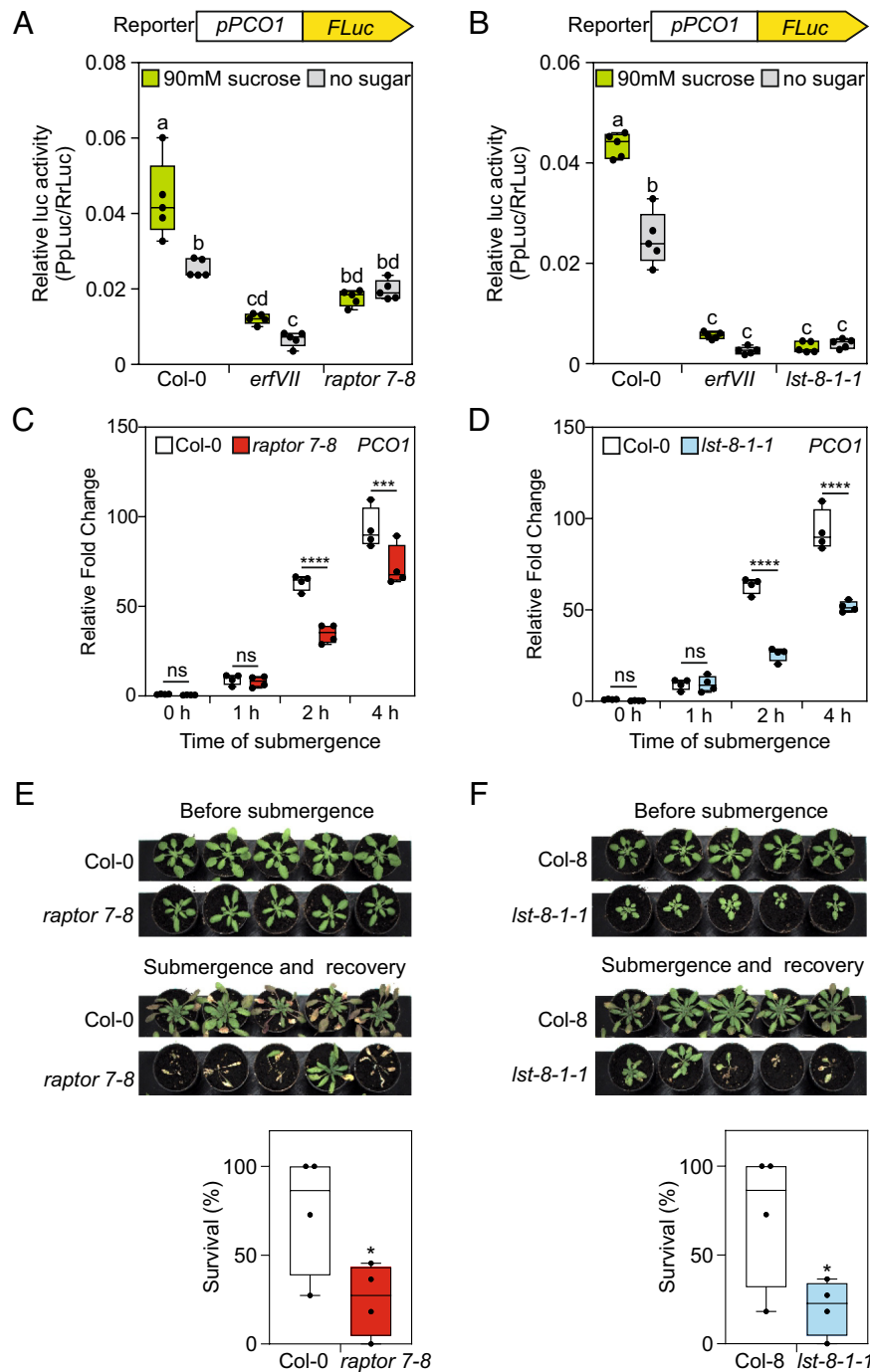


Fig. 4. TOR complex affects the strength of hypoxic responses and tolerance. (A) Relative activity of *PCO1* promoter corresponding to the strength of hypoxic responses in Col-0, *erfVII* and *raptor 7-8* protoplasts after 4-h hypoxia treatment. Half of the samples were supplied with 90 mM sucrose. (B) The same as A but with *lst-8-1-1* mutant. (C) Relative fold change of *PCO1* expression in Col-0 and *raptor 7-8* plants in air and after 1 h, 2 h, and 4 h of submergence in the dark after 6 h in the light. (D) The same as C but with *lst-8-1-1* mutant. (E) Phenotypes of Col-0 and *raptor 7-8* plants which underwent a 6-h pretreatment in the light, before and after 2 d of submergence. Photographs were taken before and after 9 d of recovery. Graph shows survival percentage assessed 9 d after submergence. (F) The same as E but with *lst-8-1-1* mutant. Data in C and D are expressed as relative to WT in air. A and B, $n = 5$ biological replicates; C and D, $n = 4$ biological replicates; E and F, $n = 4$ biological replicates (11 plants per replicate). In the boxplots, dots represent single data points, whiskers denote the minimum/maximum values, the box defines the interquartile range, the center represents the median, and box borders represent the lower and upper quartiles. Different letters (a, b, c, bd, cd) indicate differences in ANOVA tests (Tukey's post hoc test, $P < 0.05$). Asterisks indicate statistically significant differences as assessed by C and D ANOVA tests (Sidak's post hoc test, $P < 0.05$); E and F Student's t test ($P < 0.05$).

was added to the protoplasts, indicating that the sugar effect acts via TOR on the last 18 amino acids at the C terminus of RAP2.12, including two serine residues (S346 and S352) (Fig. 5 A–C). Next, we transformed *erfVII* protoplasts with full versions of *RAP2.12* under the control of its own promoter (Fig. 5 D and E). When the native coding sequence of *RAP2.12* was expressed, there was a marked induction of *pPCO1:FLuc*, used as a reporter of RAP2.12

activity as a transcription factor. On the other hand, when the RAP2.12 sequence was mutated, exchanging the serine residues with alanine (S346A, S352A), there was only a slight activation of *pPCO1:FLuc*, without any enhancing sucrose effects (Fig. 5D).

The two serine residues at the C terminus of RAP2.12 are therefore involved in the sucrose modulation of the transcriptional activity of RAP2.12. Either S346 or S352 is required for

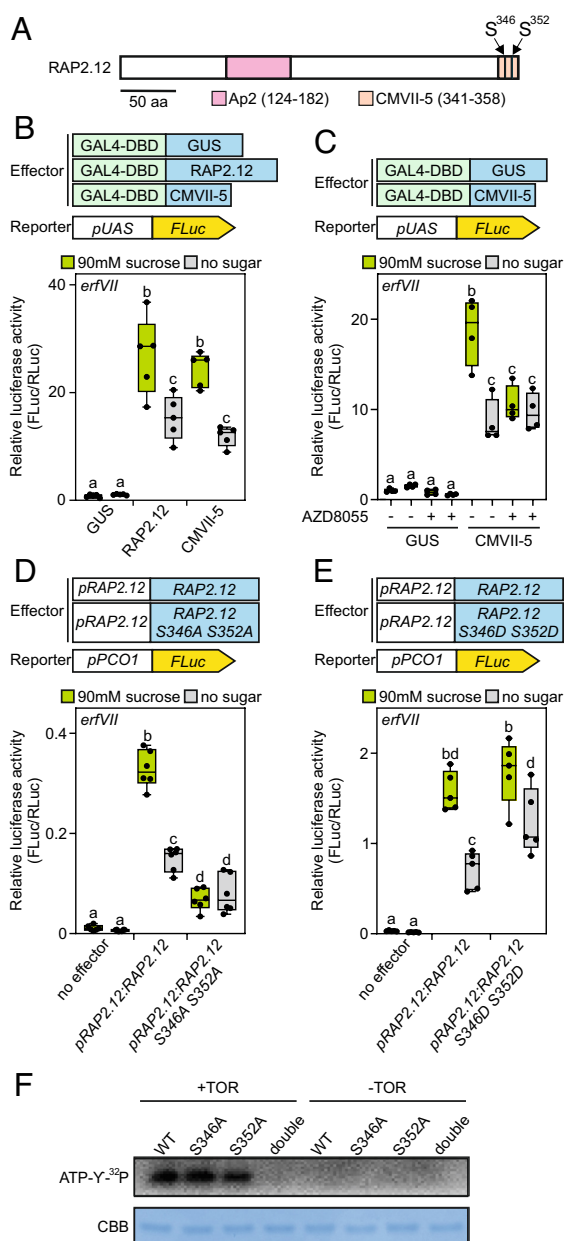


Fig. 5. Ser³⁴⁶ and Ser³⁵² residues in CMVII-5 motif are phosphorylated by TOR. (A) RAP2.12 protein with highlighted DNA-binding domain (Ap2) and activation domain (CMVII-5) containing Ser³⁴⁶ and Ser³⁵² residues. (B) Relative transcriptional activity of RAP2.12 and CMVII-5 domain fused to GAL4 DNA-binding domain in *erfVII* protoplasts after 4-h hypoxia treatment. GUS protein was used as a negative control. Half of the samples were supplied with 90 mM sucrose. Values were normalized to GUS with sucrose. (C) Effect of 1 μ M AZD8055 inhibitor on the transcriptional activity of CMVII-5 domain fused to GAL4 DNA-binding domain in *erfVII* protoplasts after 4-h hypoxia treatment. GUS protein was used as a negative control. Half of the samples were supplied with 90 mM sucrose. (D) Relative transcriptional activity of RAP2.12 and RAP2.12 protein version with Ser³⁴⁶ and Ser³⁵² residues substituted by Ala, in *erfVII* protoplasts after 4-h hypoxia treatment. Half of the samples were supplied with 90 mM sucrose. (E) The same as D but Ser³⁴⁶ and Ser³⁵² residues were substituted by Asp. (F) In vitro kinase assay of GST-fusion proteins with the C-terminal part of WT RAP2.12, either phosphosite S346A or S352A mutant and RAP2.12 with both serine residues substituted by alanine (double). Proteins were incubated with TAP-purified (tandem affinity purification) TOR kinase (+TOR) or with TAP-purified untransformed WT PSB-D cell cultures, as a negative control (-TOR). Phosphorylation of GST-RAP2.12 fusion proteins was visualized by autoradiography after 8 d of exposure. CBB staining of substrates was used to test for equal loading. B and E, $n = 5$ biological replicates; C, $n = 4$ biological replicates; D, $n = 6$ biological replicates. In the boxplots, dots represent single data points, whiskers denote the minimum/maximum values, the box defines the interquartile range, the center represents the median, and box borders represent the lower and upper quartiles. Different letters (a, b, c, d, bd) indicate differences in ANOVA tests (Tukey's post hoc test, $P < 0.05$).

conferring sucrose responsiveness to RAP2.12, given that a single substitution of S346 or S352 with S346A or S352A is sufficient to make RAP2.12 insensitive to the presence of sucrose (SI Appendix, Fig. S16). Mutation of the two C-terminal serines into aspartic acid (D) should result in constitutively active RAP2.12 as far as the phosphorylation status is concerned. This was confirmed experimentally in *erfVII* protoplasts that were transformed with a *pRAP2.12:RAP2.12 S346D S352D*, showing a strong expression of the *pPCO1* promoter even in the absence of exogenous sugars (Fig. 5E).

RAP2.12 Is Phosphorylated at Two Serine Residues by TOR Kinase. Overall, the data reported above suggest that RAP2.12 is phosphorylated by TOR in vivo, and that this phosphorylation causes the activation of RAP2.12. To test whether the S346/S352-bearing CMVII-5 activation domain of RAP2.12 could indeed be phosphorylated by TOR, we conducted an in vitro kinase assay. We purified *Escherichia coli* expressed GST-fusion proteins (Glutathione S-transferase) with the CMVII-5 motif of WT RAP2.12, with either S346 or S352 mutated to alanine (S346A and S352A) or with both serines exchanged (double). The active TOR kinase complex was purified from Arabidopsis cell cultures by tandem affinity purification of the GSRhino-tagged RAPTOR protein (35). As shown in Fig. 5F, active TOR strongly phosphorylates RAP2.12 WT and both S346 and S352 single mutant variants. By contrast, when both serines were mutated to alanine (double), TOR was unable to phosphorylate the protein (Fig. 5F), indicating that TOR can phosphorylate the C-terminal CMVII-5 motif of RAP2.12 at positions S346 and S352.

While Ser phosphorylation on the C terminus of RAP2.12 plays a role in activating the transcription of *HRGs* (Fig. 5D and E), it is unknown whether this also alters the subcellular localization of this ERF-VII. We thus verified the nuclear localization of RAP2.12 variants that have S346 and S352 individually or both converted to alanine (S346A and S352A). The results showed that the absence of these serine residues does not prevent the nuclear localization of RAP2.12 (SI Appendix, Fig. S17).

The three ERF-VII proteins primarily responsible for the hypoxic activation of *HRGs*, are the constitutively expressed RAP2.2, RAP2.3, and RAP2.12 (34). The CMVII-5 motif at the C terminus is present in RAP2.2 and RAP2.12, but absent in RAP2.3 (36). In fact, RAP2.3 lacks the S346 residue, which is instead conserved in both RAP2.2 and RAP2.12 (SI Appendix, Fig. S18A). We tested whether all three RAP proteins belonging to the ERF-VII group are sugar responsive by transforming *erfVII* protoplasts with either 35S:RAP2.12, 35S:RAP2.2 or 35S:RAP2.3. The sucrose-dependent transactivation of *pPCO1* by RAP2.12 and RAP2.2 was evident, but absent when RAP2.3 was utilized (SI Appendix, Fig. S18B). This corroborates the importance of S346 in conferring sucrose responsiveness to ERF-VII proteins. Both S346 and S352 are, however, important for the TOR-dependent activation of RAP2.12, given that even when a single serine residue is replaced with alanine, the sugar-dependent activation of RAP2.12 is lost (SI Appendix, Fig. S16). While RAP2.2 has a serine in CMVII-5 domain coinciding with the one in RAP2.12 (S367 in RAP2.2; S346 in RAP2.12), this domain in RAP2.3 only possesses one serine residue (S246; SI Appendix, Fig. S19). When S367 was converted to S367A in RAP2.2, sugar responsiveness was completely lost (SI Appendix, Fig. S19A). However, although there was a slight sucrose-dependent enhancement of RAP2.3 (SI Appendix, Figs. S18B and S19B), the mutation of S246 to S246A into RAP2.3 resulted in a comparable expression of *pPCO1:FLuc* with/without sugar, suggesting that this Ser residue is not required for the sugar-dependent regulation

of RAP2.3 (*SI Appendix, Fig. S19B*). This indicates that other mechanisms may be involved in the modest sugar regulation of RAP2.3.

Discussion

In plants, oxygen sensing relies on the hypoxia-dependent stabilization of ERF-VII, which triggers the transcriptional activation of HRGs and, ultimately, tolerance to abiotic stresses such as submergence and waterlogging (4). Among HRGs, there are several genes coding for enzymes involved in carbohydrate metabolism, such as sucrose synthases, PDC, and alcohol dehydrogenase (3–5, 37). Adaptation to hypoxia requires a reduction in energy consumption, given that ATP synthesis is severely inhibited when oxygen is a limiting factor for respiration (1). Gene expression is remodulated under hypoxia so that only those genes required for survival are active. Sugar availability acts as a positive factor to enable plants to survive hypoxia and anoxia (9, 17, 23). Importantly, higher sucrose availability enhances the messenger RNA level of HRGs (17), and sugar starvation considerably reduces the RAP2.12-dependent expression of HRGs (9). The impact of carbon starvation on RAP2.12 activity is independent of the known repressors of its activity such as HRA1 (9, 22), and is also independent of the mechanism for stabilizing RAP2.12 through the N-degron pathway (9).

Here, we have demonstrated that the sugar starvation dampening of the hypoxia response at transcriptional level is related to energy sensing. In plants, TOR acts as the central molecular switch to regulate metabolism, cell proliferation, and plant growth in response to sugars derived directly or indirectly from photosynthesis (26, 38). Sucrose and glucose are the most effective sugars that activate TOR, because glycolysis and mitochondrial bioenergetics are required for the activation of the kinase. Both these sugars activate the expression of the *pPCO1* promoter (*SI Appendix, Fig. S11C*). Notably, inhibiting photosynthesis using DCMU or mitochondrial ATP production by oligomycin inhibited TOR activity (*SI Appendix, Fig. S7*) and resulted in the reduced induction of HRGs (Fig. 1 and *SI Appendix, Figs. S4 and S5*). Similarly, specific ATP-competitive TOR inhibitors also repressed HRG induction (Fig. 3D).

Interestingly, inhibition of photosynthesis by darkness or DCMU in *Chlamydomonas* led to a gradual and pronounced decrease in TOR activity (39). Darkness, as well as submergence in the dark, considerably reduced TOR activity (Fig. 2A). However, RAP2.12 activity relies on the presence of active TOR for the induction of HRGs, as demonstrated by the experiments in which TOR is genetically or chemically inhibited (Fig. 3 and *SI Appendix, Figs. S8–S10*). Therefore, darkness (which reduces the availability of ATP in the cell) results in the inactivation of TOR (Fig. 2), which is required in its active status to induce HRGs (Fig. 2). The action of TOR on the mechanism by which HRGs are induced seems to rely on the phosphorylation of the C-terminal activation domain of RAP2.12 at S346 and S352 positions (Fig. 5F). Given that we excluded an involvement of SnRK1 downstream of TOR (9), we cannot rule out that the negative impact of submergence on the activity of TOR is due to limited ATP availability (Fig. 2), although the TOR activity kept declining even when the submerged plants reached a steady state in their ATP content (Fig. 2E).

A low level of ATP is therefore a signal for reduced HRG expression under hypoxia, via TOR signaling. An extended night treatment alone is very effective in reducing the ATP level, regardless of oxygen availability (Fig. 1E and H). Furthermore, even plants that were submerged in the dark after a period under light

underwent a drop in ATP content (Fig. 2E), correlating with the gradually reduced activity of TOR (Fig. 2B). This suggests that the drop in expression of HRGs observed after a few hours of hypoxia (Fig. 1A) is due to insufficient activity of TOR acting as an activator of RAP2.12 through phosphorylation of two serine residues located in the activation domain of this transcription factor (Fig. 5).

Low-ATP has been proposed as being a part of the overall oxygen sensing mechanism. Briefly, a drop in ATP at the onset of dark hypoxia induces a change in the oleoyl-CoA levels leading to dissociation of RAP2.12 from the plasma membrane and translocation to the nucleus when the oxygen level is sufficiently low to prevent the PCO-dependent degradation of RAP2.12 (16).

A low level of ATP therefore contributes to the induction of HRGs, yet our results indicated that a low level of ATP dampens the HRG induction via the inactivation of TOR signaling. These results are not contradictory given that the levels of *ADH1* induction recorded in our experiments under low ATP levels (~40-fold induction by hypoxia) are comparable to the fold induction of *ADH1* observed by Schmidt et al. (16) under similarly low ATP levels. Basically, when the ATP level is kept high, the induction of *ADH1* by hypoxia is several times greater than under low ATP (Fig. 1).

Through our tests, we ruled out the possibility that a dark pre-treatment or even inhibition of TOR by AZD8055 negatively affects the ERF-VII protein level (9). Instead, we found that darkness, DCMU, and AZD8055 treatments all enhanced the nuclear localization of RAP2.12 (*SI Appendix, Fig. S12*). This indicates that sugar/energy starvation conditions, as well as the inhibition of TOR, enhance the nuclear localization of RAP2.12, similarly to the finding described for another ethylene-related protein, namely EIN2 (40). Ethylene triggers the dephosphorylation of EIN2, which defines its nuclear accumulation. Inhibition of TOR has been found to enhance the nuclear localization of EIN2 from various species, indicating that TOR-mediated phosphorylation of EIN2 prevents its nuclear localization (40). We found that a high energy status activated TOR, which thus appeared to limit the translocation of RAP2.12 to the nucleus. However, the activation of a smaller amount of nuclear localized RAP2.12 by TOR activity, ensures a sufficient production of HRGs. Conversely, if RAP2.12 is relatively inactive due to the presence of AZD8055, its amount in the nucleus increases, possibly to compensate for the lower activity of the transcription factor (TF) (*SI Appendix, Fig. S12*). The dynamics of RAP2.12 localization to the nucleus subjected to its TOR-dependent activation status suggest the existence of a mechanism regulating the translocation of RAP2.12 to the nucleus with an efficiency, which is inversely correlated to its activity.

In animal cells, mTOR is an upstream activator of the oxygen sensor HIF-1 (hypoxia inducible factor) (41). Rapamycin is an inhibitor of TOR, and unlike what was initially proposed (41), it does not affect the stability of HIF-1 α . Instead, it modulates HIF activity via a Von Hippel–Lindau-independent mechanism (42). Similarly, low-energy has not been found to impact the stability of the plant's RAP2.12 oxygen sensor via the N-degron pathway (9). Rapamycin-sensitive functions of mTOR in animal cells have been shown to be dispensable for the accumulation of HIF-1 α but are required for optimal HIF-1-dependent gene expression under hypoxic conditions (42).

Our results indicate that in plants, AZD8055-sensitive functions of TOR are also required for optimal ERF-VII-dependent gene expression under hypoxia (Fig. 3). Although oxygen-sensing mechanisms in animals and plants use unrelated TFs, they clearly show many mechanistical similarities (43). We found that they also share a strategy for coordinating responses to hypoxia with the energy status of the cell. This highlights how important it is

for complex organisms to relate anaerobic metabolism with the availability of resources.

Materials and Methods

Plant Material and Growth Conditions. *Arabidopsis thaliana* ecotype Columbia (Col-0) was used as the WT ecotype for all experiments, unless stated otherwise. The genotypes used in this manuscript include the quintuple *erfVII* mutant (44), the ethanol-inducible *TOR RNAi* 6-3 line (45), the *raptor* 7-8 mutant (46), the *lst8-1-1* (47) mutant, and *35S::Δ13RAP2.12-GFP* line (12). The estradiol-inducible *TOR RNAi* line (*tor-es2*) was obtained from Nottingham Arabidopsis Stock Centre (N69830) (31).

Plant growth conditions are explained in detailed in *SI Appendix*.

Inhibitor and Chemical Treatments. Chemical compounds were either sprayed on plants grown in pots or added directly to the protoplast solutions. The complete procedures are included in *SI Appendix*.

Total RNA Extraction and Real-Time qPCR Analysis. Total RNA extraction, DNase treatment, cDNA synthesis, and qRT-PCR analysis were performed as previously described (48). A complete list of primers used in qRT-PCR analysis is shown in *SI Appendix, Table S1*.

Construct Preparation. Entry clones for *RAP2.2* (34), *RAP2.3* (34), and *RAP2.12* (15) coding sequences, and *pPCO1* promoter (15) were available in our facility. Remaining entry clones were generated by site-directed mutagenesis. The entry vectors were recombined into destination vectors using the LR reaction mix II (Thermo-Fisher Scientific) to get the corresponding expression vectors.

Detailed preparation of *RAP2.12* constructs driven by its native promoter and constructs used for protein expression is included in *SI Appendix*. A complete list of primers and vectors used for the cloning is included in *SI Appendix, Tables S2 and S3*.

Protein Extraction, SDS-PAGE, Immunoblotting and Band Intensity Quantification. Total protein extracts were obtained from 4-wk-old Arabidopsis rosettes or 6 mL WI solution containing protoplasts, following the protocol presented in *SI Appendix*.

Protoplast Isolation and Transformation. Arabidopsis mesophyll protoplasts were isolated and transformed as previously described (49). Detailed protocol is provided in *SI Appendix*.

Luciferase Activity Quantification. Firefly (*Photinus pyralis*) and *Renilla reniformis* luciferase activities were assessed using the Dual-Luciferase Reporter Assay System (Promega) for transactivation assays, following the company protocol. The

firefly luciferase activity was normalized to *Renilla* luciferase activity using the Lumat LB 9507 Tube Luminometer (Berthold).

Transient Transfection of *Nicotiana benthamiana*. Transient transfection with *Agrobacterium tumefaciens* cultures was performed as previously described (50).

Confocal Microscopy. Imaging of *35S::Δ13RAP2.12-GFP* Arabidopsis line and transiently transfected *Nicotiana benthamiana* leaves was carried out using a Zeiss Airyscan 800 confocal microscope. Leaves from 4-wk-old independent plants were imaged at the end of each treatment as indicated in the figure legend. GFP and chlorophyll signals were detected using 488-nm laser light and collected at 492 to 547 and 645 to 700 nm, respectively. ZEN BLUE software (Carl Zeiss) was used to quantify *35S::Δ13RAP2.12-GFP* fluorescence intensity.

Extraction and Analysis of Carbohydrates. Four-week-old rosettes were harvested and flash frozen in liquid nitrogen. Homogenized samples were then extracted in 80% ethanol. Glucose, fructose, and sucrose were measured enzymatically in soluble fraction (51). Starch was assessed in the insoluble pellet (52).

ATP Assay. Plant material was extracted by grinding pre-cooled samples in liquid nitrogen to a fine powder. Detailed protocol is presented in *SI Appendix*.

Protein Expression and Purification. Expression and purification of GST-fusion proteins were performed as described in detail in *SI Appendix*.

In Vitro Kinase Assay. TOR kinase complex was purified as previously described (35). Details of kinase assay are provided in *SI Appendix*.

Statistical Analysis. Data were analyzed using one-way, two-way, and three-way ANOVA tests (Sidak's, Tukey's, or Dunnett's post hoc test, $P < 0.05$). Pairwise comparisons were performed by Student's, Kruskal-Wallis, or Mann-Whitney's *t* test.

Data, Materials, and Software Availability. All study data are included in the article and/or *SI Appendix*.

ACKNOWLEDGMENTS. This work was supported by Sant'Anna School of Advanced Studies, Pisa.

Author affiliations: ^aPlantLab, Center of Plant Sciences, Sant'Anna School of Advanced Studies, 56010 Pisa, Italy; ^bDepartment of Plant Physiology, Rheinisch-Westfälische Technische Hochschule Aachen University, 52074 Aachen, Germany; ^cInstitut Jean-Pierre Bourgin, Institut National de la Recherche Agronomique-AgroParisTech, Université Paris-Saclay, 78000 Versailles, France; ^dDepartment of Plant Biotechnology and Bioinformatics, Ghent University, 9052 Ghent, Belgium; ^eVlaams Instituut voor Biotechnologie, Center for Plant Systems Biology, 9052 Ghent, Belgium; ^fPlant-Environment Signaling, Institute of Environmental Biology, Utrecht University, 3584 CH Utrecht, The Netherlands; ^gnanoplant Center @NEST, Institute of Life Sciences, Scuola Superiore Sant'Anna, 56127 Pisa, Italy; and ^hInstitute of Agricultural Biology and Biotechnology, National Research Council, 56124 Pisa, Italy

1. T. Fukao, J. Bailey-Serres, Plant responses to hypoxia—Is survival a balancing act? *Trends Plant Sci.* **9**, 449–456 (2004).
2. J. Bailey-Serres, L. A. C. J. Voesenek, Flooding stress: Acclimations and genetic diversity. *Annu. Rev. Plant Biol.* **59**, 313–339 (2008).
3. E. Loreti, P. Perata, The many facets of hypoxia in plants. *Plants* **9**, 745 (2020).
4. E. Loreti, H. van Veen, P. Perata, Plant responses to flooding stress. *Curr. Opin. Plant Biol.* **33**, 64–71 (2016).
5. P. Perata, A. Alpi, Plant responses to anaerobiosis. *Plant Sci.* **93**, 1–17 (1993).
6. M. Mithran, E. Paparelli, G. Novi, P. Perata, E. Loreti, Analysis of the role of the pyruvate decarboxylase gene family in *Arabidopsis thaliana* under low-oxygen conditions. *Plant Biol.* **16**, 28–34 (2014).
7. K. P. Ismond, R. Dolferus, M. De Pauw, E. S. Dennis, A. G. Good, Enhanced low oxygen survival in *Arabidopsis* through increased metabolic flux in the fermentative pathway. *Plant Physiol.* **132**, 1292–1302 (2003).
8. I. Ventura *et al.*, Arabidopsis phenotyping reveals the importance of alcohol dehydrogenase and pyruvate decarboxylase for aerobic plant growth. *Sci. Rep.* **10**, 16669 (2020).
9. E. Loreti, M. C. Valeri, G. Novi, P. Perata, Gene regulation and survival under hypoxia requires starch availability and metabolism. *Plant Physiol.* **176**, 1286–1298 (2018).
10. P. Gasch *et al.*, Redundant ERF-VII transcription factors bind to an evolutionarily conserved cis-motif to regulate hypoxia-responsive gene expression in arabidopsis. *Plant Cell* **28**, 160–180 (2016).
11. B. Giuntoli, P. Perata, Group VII ethylene response factors in arabidopsis: Regulation and physiological roles. *Plant Physiol.* **176**, 1143–1155 (2018).
12. F. Licausi *et al.*, Oxygen sensing in plants is mediated by an N-end rule pathway for protein destabilization. *Nature* **479**, 419–422 (2011).
13. D. J. Gibbs *et al.*, Homeostatic response to hypoxia is regulated by the N-end rule pathway in plants. *Nature* **479**, 415–418 (2011).
14. S. Hartman *et al.*, Ethylene-mediated nitric oxide depletion pre-adapts plants to hypoxia stress. *Nat. Commun.* **10**, 1–9 (2019).
15. D. A. Weits *et al.*, Plant cysteine oxidases control the oxygen-dependent branch of the N-end rule pathway. *Nat. Commun.* **5**, 1–10 (2014).
16. R. R. Schmidt *et al.*, Low-oxygen response is triggered by an ATP-dependent shift in oleoyl-CoA in *Arabidopsis*. *Proc. Natl. Acad. Sci. U.S.A.* **115**, E312101–E312110 (2018).
17. E. Loreti, A. Poggi, G. Novi, A. Alpi, P. Perata, A genome-wide analysis of the effects of sucrose on gene expression in arabidopsis seedlings under anoxia. *Plant Physiol.* **137**, 1130–1138 (2005).
18. A. Mustroph *et al.*, Cross-kingdom comparison of transcriptomic adjustments to low-oxygen stress highlights conserved and plant-specific responses. *Plant Physiol.* **152**, 1484–1500 (2010).
19. L. T. Bui *et al.*, Conservation of ethanol fermentation and its regulation in land plants. *J. Exp. Bot.* **70**, 1815–1827 (2019).
20. S. C. Lee *et al.*, Molecular characterization of the submergence response of the *Arabidopsis thaliana* ecotype Columbia. *New Phytol.* **190**, 457–471 (2011).
21. K. Xu *et al.*, Sub1A is an ethylene-response-factor-like gene that confers submergence tolerance to rice. *Nature* **442**, 705–708 (2006).
22. B. Giuntoli *et al.*, A trihelix DNA binding protein counterbalances hypoxia-responsive transcriptional activation in Arabidopsis. *PLoS Biol.* **12**, e1001950 (2014).
23. H. Cho, E. Loreti, M. Shih, P. Perata, Energy and sugar signaling during hypoxia. *New Phytol.* **229**, 57–63 (2021).
24. C. Robaglia, M. Thomas, C. Meyer, Sensing nutrient and energy status by SnRK1 and TOR kinases. *Curr. Opin. Plant Biol.* **15**, 301–307 (2012).
25. A. Kravchenko *et al.*, Mutations in the Arabidopsis *Lst8* and *Raptor* genes encoding partners of the TOR complex, or inhibition of TOR activity decrease abscisic acid (ABA) synthesis. *Biochem. Biophys. Res. Commun.* **467**, 992–997 (2015).
26. G. M. Burkart, F. Brandizzi, A tour of TOR complex signaling in plants. *Trends Biochem. Sci.* **46**, 417–428 (2021).
27. D. J. Price, J. R. Grove, V. Calvo, J. Avruch, B. E. Bierer, Rapamycin-induced inhibition of the 70-kilodalton S6 protein kinase. *Science* **257**, 973–977 (1992).

28. M.-H. Montané, B. Menand, ATP-competitive mTOR kinase inhibitors delay plant growth by triggering early differentiation of meristematic cells but no developmental patterning change. *J. Exp. Bot.* **64**, 4361–4374 (2013).
29. M. M. Mahfouz, S. Kim, A. J. Delauney, D. P. S. Verma, Arabidopsis TARGET of RAPAMYCIN interacts with RAPTOR, which regulates the activity of S6 kinase in response to osmotic stress signals. *Plant Cell* **18**, 477–490 (2006).
30. C. M. Pereyra, N. R. Aznar, M. S. Rodriguez, G. L. Salerno, G. M. A. Martínez-Noël, Target of rapamycin signaling is tightly and differently regulated in the plant response under distinct abiotic stresses. *Planta* **251**, 21 (2019).
31. Y. Xiong, J. Sheen, Rapamycin and glucose-target of rapamycin (TOR) protein signaling in plants. *J. Biol. Chem.* **287**, 2836–2842 (2012).
32. M. Abbas *et al.*, Oxygen sensing coordinates photomorphogenesis to facilitate seedling survival. *Curr. Biol.* **25**, 1483–1488 (2015).
33. T. Dobrenel *et al.*, TOR signaling and nutrient sensing. *Annu. Rev. Plant Biol.* **67**, 261–285 (2016).
34. L. T. Bui, B. Giuntoli, M. Kosmacz, S. Parlanti, F. Licausi, Constitutively expressed ERF-VII transcription factors redundantly activate the core anaerobic response in Arabidopsis thaliana. *Plant Sci.* **236**, 37–43 (2015).
35. J. Van Leene *et al.*, Capturing the phosphorylation and protein interaction landscape of the plant TOR kinase. *Nat. Plants* **5**, 316–327 (2019).
36. T. Nakano, K. Suzuki, T. Fujimura, H. Shinshi, Genome-wide analysis of the ERF gene family in Arabidopsis and rice. *Plant Physiol.* **140**, 411–432 (2006).
37. A. Santaniello, E. Loreti, S. Gonzali, G. Novi, P. Perata, A reassessment of the role of sucrose synthase in the hypoxic sucrose-ethanol transition in Arabidopsis. *Plant Cell Environ.* **37**, 2294–2302 (2014).
38. Y. Wu *et al.*, Integration of nutrient, energy, light, and hormone signalling via TOR in plants. *J. Exp. Bot.* **70**, 2227–2238 (2019).
39. M. J. Mallen-Ponce, M. E. Perez-Perez, J. L. Crespo, Photosynthetic assimilation of CO₂ regulates TOR activity. *Proc. Natl. Acad. Sci. U.S.A.* **119**, e2115261119 (2022).
40. L. Fu *et al.*, The TOR-EIN2 axis mediates nuclear signalling to modulate plant growth. *Nature* **591**, 288–292 (2021).
41. C. C. Hudson *et al.*, Regulation of hypoxia-inducible factor 1 α expression and function by the mammalian target of rapamycin. *Mol. Cell. Biol.* **22**, 7004–7014 (2002).
42. S. C. Land, A. R. Tee, Hypoxia-inducible factor 1 α is regulated by the mammalian target of rapamycin (mTOR) via an mTOR signaling motif. *J. Biol. Chem.* **282**, 20534–20543 (2007).
43. F. Licausi, B. Giuntoli, P. Perata, Similar and yet different: Oxygen sensing in animals and plants. *Trends Plant Sci.* **25**, 6–9 (2020).
44. N. Marín-de La Rosa *et al.*, Large-scale identification of gibberellin-related transcription factors defines group VII ethylene response factors as functional DELLA partners. *Plant Physiol.* **166**, 1022–1032 (2014).
45. D. Deprost *et al.*, The Arabidopsis TOR kinase links plant growth, yield, stress resistance and mRNA translation. *EMBO Rep.* **8**, 864–870 (2007).
46. D. Deprost, H. N. Truong, C. Robaglia, C. Meyer, An Arabidopsis homolog of RAPTOR/KOG1 is essential for early embryo development. *Biochem. Biophys. Res. Commun.* **326**, 844–850 (2005).
47. M. Moreau *et al.*, Mutations in the Arabidopsis homolog of LST8/G β L, a partner of the target of rapamycin kinase, impair plant growth, flowering, and metabolic adaptation to long days. *Plant Cell* **24**, 463–481 (2012).
48. F. Betti *et al.*, Exogenous miRNAs induce post-transcriptional gene silencing in plants. *Nat. Plants* **7**, 1379–1388 (2021).
49. S. Iacopino *et al.*, A synthetic oxygen sensor for plants based on animal hypoxia signaling. *Plant Physiol.* **179**, 986–1000 (2019).
50. G. Panicucci, S. Iacopino, E. De Meo, P. Perata, D. A. Weits, An improved HRPE-based transcriptional output reporter to detect hypoxia and anoxia in plant tissue. *Biosensors* **10**, 197 (2020).
51. L. Guglielminetti, P. Perata, A. Alpi, Effect of anoxia on carbohydrate metabolism in rice seedlings. *Plant Physiol.* **108**, 735–741 (1995).
52. J. H. Critchley, S. C. Zeeman, T. Takaha, A. M. Smith, S. M. Smith, A critical role for disproportionating enzyme in starch breakdown is revealed by a knock-out mutation in Arabidopsis. *Plant J.* **26**, 89–100 (2001).